Mech Time-Depend Mater (2015) 19:277–304
DOI 10.1007/s11043-015-9264-x

Vibration behavior of a viscoelastic composite microbeam under simultaneous electrostatic and piezoelectric actuation

F. Chitsaz Yazdi[1] · A. Jalali[1]

Received: 2 February 2014 / Accepted: 6 April 2015 / Published online: 19 May 2015

Abstract In this paper, the static and dynamic response of a clamped–clamped viscoelastic nanocomposite microbeam under combined electrostatic and piezoelectric actuations is analyzed. The equations of motion of the system are derived using the Euler–Bernoulli beam theory, Kelvin–Voigt model and Hamilton principle. The nonlinear model for the system is studied by considering stretching of the mid-plane, a DC electrostatic force, an AC harmonic force and a DC piezoelectric actuation. The static deflection and natural frequency of the system is extracted, and the influence of system parameters on the primary resonance behavior of the system is studied. It is shown that, based on various electrostatic and piezoelectric excitations, hardening or softening behavior is expected. So, one can tune these voltages such that this highly nonlinear system behaves linearly close to resonance frequency. Also it is shown that damping characteristics of the system with viscoelastic material not only depends on the damping coefficient of the system, but also on its other parameters.

Keywords Composite microbeam · Multiple scale method · Viscoelastic · Piezoelectric layer · Electrostatic

List of Abbreviation

$A(T_1, T_2)$	Complex-valued function for system response with amplitude a and phase ϑ
A_1	Cross-section of the microbeam
A_2	Cross-section of the piezoelectric layer
$B_c(t)$	Constant of integration
$B_1(s)$, $B_3(s)$	The axial and bending stiffness of the system, respectively
$B_2(s)$, $B_4(s)$	The axial load and bending moment due to the piezoelectric effects, respectively
$B_5(s)$, $B_6(s)$	The axial load and bending moment due to viscoelastic effect
C	Viscoelastic damping coefficient
$C_i, i = 1, \dots, 4$	Coefficients of the solution equation $\varphi_{s[i]}$

✉ A. Jalali
amirjalali@shahroodut.ac.ir

[1] Department of Mechanical Engineering, University of Shahrood, Shahrood, Iran

d_{31}	Piezoelectric constant
E_1	Microbeam modulus of elasticity
E_2	Piezoelectric modulus of elasticity
e	The axial strain of the microbeam
F	The external force due to AC actuation
$\hat{f}$	Constant displacement applied to the one end of the microbeam
$g_i, i = 1, 2$	The positive roots of the characteristic equation governed by $\varphi_{s[i]}$
$H_{1n}(x)$	Dimensionless coefficient of the linear term due to bending stiffness of the system
$H_{2n}(x)$	Dimensionless coefficient of the linear term due to viscoelastic effects
$H_{3n}(x)$	Dimensionless coefficient of the nonlinear term due to viscoelastic effects
H_{l_i}	Heaviside function at the point l_i
h	Initial gap
I_1	Second moment of the area of the microbeam about the neutral axis for $s < l_1$ or $s > l_2$
I_2	Second moment of the area of the piezoelectric layer about the neutral axis for $l_1 < s < l_2$
I_3	Second moment of the area for the cross-section of the microbeam about the neutral axis for $l_1 < s < l_2$
K	Kinetic energy
L	Length of the microbeam
$l_2 - l_1$	Length of the piezoelectric layer
$M(s)$	Mass per unit length of the microbeam
$M_n(x)$	Dimensionless mass per unit length of the system
P	Distance between the neutral axis and the mid-plane of the microbeam for $l_1 < s < l_2$
Q	Electrostatic force
R_1, R_2	The positive roots of the characteristic equation governed by $\varphi_{s[i]}$
s	Position along the length of the microbeam
$T_i, i = 0, 1, 2$	Time scales
t_1	Thickness of the microbeam
t_2	Thickness of the piezoelectric layer
U	Potential energy
$u(x, \tau)$	Dimensionless form of the dynamic deflection
V	Longitudinal displacement
v_{ac}	AC fluctuation voltage between the microbeam and the stationary electrode
v_{dc}	DC polarization voltage between the microbeam and the stationary electrode
v_P	DC voltage between the upper and lower surface of the piezoelectric layer
v_1	Length of the microbeam
v_2	Length of the piezoelectric layer
W	Transverse displacement
w	Dimensionless form of W
w_c	Width of the microbeam and the piezoelectric layer
w_s	Dimensionless static deflection
$X_i, i = 1, \ldots, 4$	Coefficients of the solution equation $\varphi_{d[i]}$
x	Dimensionless form of s
α	Dimensionless measure of the axial load

γ	Dimensionless measure of the piezoelectric actuation
γ_{P1}	Dimensionless measures of the axial load due to the piezoelectric effects
γ_{P2}	Dimensionless measures of the bending moment due to the piezoelectric effect
δ_{1i}	Kronecker delta
ε	Small dimensionless bookkeeping parameter
ε_s	Strain of the microbeam
ε_0	Dielectric constant of the medium
η	Dimensionless measure of the electrostatic actuation
κ	Curvature bending of the microbeam in the sz plane
μ	Damping coefficient of the viscoelastic microbeam
ρ_1	Specific density of the microbeam
ρ_2	Specific density of the piezoelectric layer
σ	Detuning parameter
σ_1	Axial stress of the microbeam
σ_2	Axial stress of the piezoelectric layer
τ	Dimensionless form of t
φ	Mode shape of the system
$\phi(x)$	Normalized linear mode shape of the microbeam
χ_q^e, χ_c^e	Electrostatic nonlinear quadratic and cubic terms
χ_q^g, χ_c^g	Geometrical nonlinear quadratic and cubic terms
$\hat{\Omega}$	Electrostatic actuation frequency
ω	Natural frequency of the system

1 Introduction

Batch fabrication, small size, low price, energy consumption, and high durability have caused the MEMS devices to be widely used in the past two decades in many scientific research fields such as biotechnological, aerospace, automotive, medical, signal processing, robotic and manufacturing (Younis 2011; Senturia 2001). Among many elements which are used as the basis of microstructures, microbeams have received great attention due to their widespread applications (Ghayesh et al. 2013a, 2013b). The nature of these structures introduces an evident coupling between electrical and mechanical behavior of the system which is not ignorable. Due to the importance and wide application of microbeam-based microstructures, many analytical/numerical analyses from various viewpoints, considering various configurations of the microbeam with different load types, were performed, and applicable results were extracted. For example, the static deflection and instability of the nonlinear micro/nano cantilever beam with tip mass was studied by Mojahedi et al. (2010). Using a homotopy perturbation method, they investigated the effects of van der Waals and Casimir forces on the static deflection and pull-in instability of the system. In another study, Ghayesh et al. (2013a, 2013b) employed the modified couple stress theory to investigate the nonlinear size-dependent resonant behavior of an electrically actuated clamped–clamped microbeam. They investigated the static and dynamic behavior of the system by means of the pseudo-arc length continuation technique.

Other researchers considered other aspects of this basic structure such as nonlinear resonant behavior (Kim et al. 2012) and nonlinear dynamics (Kacem et al. 2011) of the microbeam resonator.

One of the inherent phenomena which appear in these devices is the pull-in phenomenon. In many applications such as resonators, it is necessary to work in the region far from the pull-in instability. Piezoelectric materials are one of the best candidates to control the behavior of the microdevices. In recent years, the applications of the smart materials such as piezoelectric materials have received serious attention. The piezoelectric materials are light, they can be easily attached on the structure, are able to provide rapid response through electromechanical coupling, and have high ability in reducing vibrations (Rezazadeh et al. 2009). So, the response analysis of the microsystems with the presence of the piezoelectric material is of great interest.

A microbeam under piezoelectric actuation was studied by Rezazadeh et al. (2009). They applied a voltage on the piezoelectric layers which were bonded on the surfaces of the microbeam and calculated the critical piezoelectric force for avoiding of the instability in the microcantilever beam and clamped–clamped microbeam. They validated the results by known buckling capacity of the Beck column.

The nonlinear response of an inhomogenous piezoelectrically actuated microcantilever beam was derived by Mahmoodi and Jalili (2007) using the multiple scale method. They considered inextensibility conditions for the microbeam.

The nonlinear response of a microcantilever beam under electrostatic and piezoelectric actuation was investigated by Chen et al. (2013). They considered the Euler–Bernoulli hypothesis and used a developed periodicity-ratio (PR) approach to analyze the behavior of the system. They considered the effects the of moment, shear, damping and axial forces in equations.

In another work, a micro-switch as a microcantilever beam was investigated under combination of electrostatic and piezoelectric actuation by Raeisifard et al. (2014). They considered nonlinearities due to inertia, curvature, electrostatic forces, and piezoelectric actuator.

Also, many other researches were performed by considering the influence of the piezoelectric patch (Ghazavi et al. 2010; Hosseinzadeh and Ahamadian 2010; Rezazadeh et al. 2006; Zamanian and Khadem 2010).

In fact, the force required for a given deformation corresponds to the stiffness of the structure, and the natural frequency of vibration is a measure of the response time. Commonly, increasing the stiffness reduced to decreasing the response time and vice versa. On the other hand, vibration with high frequency (low response time) and large amplitude (low stiffness) is one of the most favorable characteristics for MEMS applications (Senturia 2001). Among many materials, composite materials have good and favorable characteristics and, among them, CNT reinforced nanocomposite materials are the best with properties rivaling those of other materials (Ashrafi et al. 2006), which is the consequence of small size and exceptional mechanical properties (Qian et al. 2002).

The static and dynamic responses of a viscoelastic microplate under combined electrostatic and piezoelectric actuations were studied by Fu and Zhang (2009). They considered the standard solid model and von Karman's plate theory for studying voltage control behavior.

In another paper, Fu et al. (2009) investigated nonlinear dynamic stability for an electrically actuated clamped–guided viscoelastic microbeam. Considering the standard linear solid model, the Euler–Bernoulli hypothesis and the Galerkin method, they investigated the effect of the environmental and inner damping, geometric nonlinear creep quantity and the symmetric electrostatic load on the principal region of instability.

The deflection, natural frequency and damping quality factor of a viscoelastic microplate under an electrostatic actuation were investigated by Jalali and Khadem (2010). They assumed a CNT-reinforced nanocomposite microplate, with electrostatic actuation applied on it and obtained static pull-in instability of the microplate.

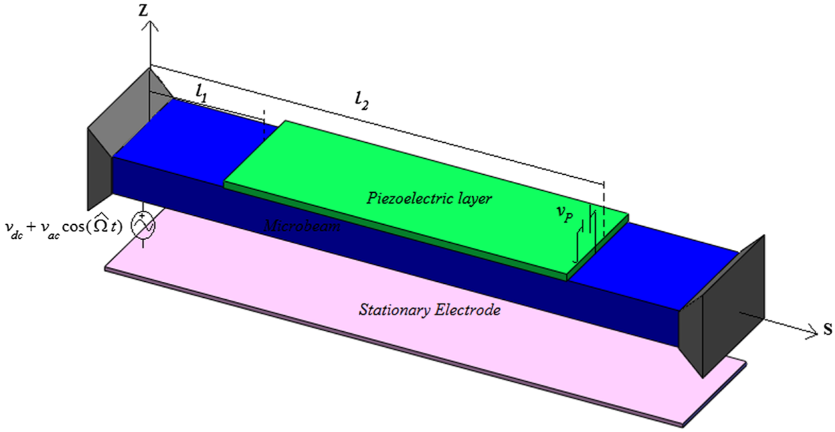

Fig. 1 Schematic of an electrostatically actuated microbeam with piezoelectric layer

Also, the response of a resonant viscoelestic clamped–clamped microbeam under electric actuation was studied by Zamanian et al. (2010). Considering mid-plane stretching, they solved a nonlinear dynamic equation using multiple scale and Galerkin methods.

Nonlinear free vibrations of viscoelastic microcantilevers with a piezoelectric actuator layer were investigated by Shooshtari et al. (2012). In this study, the microcantilever complies with the Euler–Bernoulli beam theory and Kelvin–Voigt model. Then, the Galerkin approximation is utilized for separation of time and displacement variables, and finally, using the method of multiple scales, the analytical relations for nonlinear natural frequency and amplitude of the vibration are derived.

The viscoelastic materials have almost high damping characteristics which make these materials an inappropriate choice for some applications.

In this paper, a geometrically nonlinear microbeam is considered taking into account the simultaneous viscous, electrostatic and piezoelectric effects, and the influence of the viscoelastic damping on the nonlinear forced response of the system as well as other parameters is studied. For this purpose, the system is considered as a clamped–clamped CNT reinforced microbeam under combination of electrostatic and piezoelectric actuations. In this study, the nonlinear Euler–Bernoulli beam theory and Kelvin–Voigt viscoelastic model are implemented, and the effect of mid-plane stretching is considered. The material properties of the viscoelastic material are derived by using the Eshelby–Mori–Tanaka method (Chen and Cheng 1996). The equations of motion are extracted using Hamilton's energy principle and then these equations are solved by using the directly applied multiple scale perturbation method and Galerkin procedure. Finally, the influence of the damping on the nonlinear response of the system is investigated.

2 Mathematical modeling

As shown in Fig. 1, in this paper a clamped–clamped uniform microbeam with constant geometrical and material properties is considered, in which L is the length, and w_c is the width of the microbeam. The microbeam is simultaneously under a combination of electrostatic and piezoelectric actuation. Electrostatic actuation is defined by $v_{dc} + v_{ac}\cos(\hat{\Omega} t)$, where v_{dc} is the DC polarization voltage, v_{ac} is the amplitude of the applied AC voltage, and $\hat{\Omega}$ is

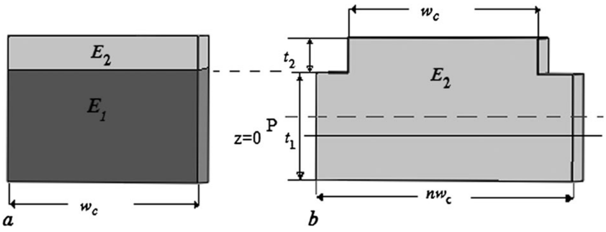

Fig. 2 (**a**) Original cross-section of microbeam and piezoelectric, (**b**) equivalent cross-section of part (**a**)

the actuation frequency. Also, piezoelectric actuation is expressed as v_P, a DC voltage, that is applied to upper and lower sides of the piezoelectric layer. Compared with the length of the microbeam, it is assumed that the air gap is very small.

Also, it is assumed that the microbeam follows the Euler–Bernoulli beam theory in which rotary inertia and shear deformation are traditionally neglected. Hamilton's principle is used to derive the governing equation of motion of the system. So, the kinetic energy of the system can be calculated as

$$K = \frac{1}{2}\int_0^L M(s)\big(\dot{V}^2 + \dot{W}^2\big)\,ds \tag{1}$$

where s is the position along the length of the microbeam and $M(s)$ is mass per unit length of the microbeam which can be obtained as

$$M(s) = w_c\rho_1 t_1 + (H_{l_1} - H_{l_2})w_c\rho_2 t_2 \tag{2}$$

where ρ_1 and ρ_2 are the specific densities of the microbeam and piezoelectric layer, respectively, w_c is the width of microbeam and the piezoelectric layer, and t_1 and t_2 are the thicknesses of the microbeam and the piezoelectric layer, respectively. In order to add the mass of the piezoelectric layer to the microbeam, a Heaviside function is used that is represented by H_{l_i} and expressed as follows:

$$H_{l_i} = \mathit{Heaviside\ function}\ (s - l_i) = \begin{cases} 1, & s > l_i, \\ 0, & s < l_i. \end{cases} \tag{3}$$

As the piezoelectric layer is attached just to the part of the microbeam length, the neutral axis changes for each section of the microbeam. For $s < l_1$ and $s > l_2$ where the piezoelectric layer does not exist, the neutral axis is the same as the geometric center of the microbeam's cross-section. But for $l_1 < s < l_2$, where the piezoelectric layer exists, the neutral axis is a distance P from the center of the microbeam. According to Timoshenko (1940), by introducing $n = \frac{E_1}{E_2}$, where E_1 and E_2 are the Young's moduli of the microbeam and the piezoelectric layer, respectively, and, by considering Fig. 2, one can obtain

$$P\sum_i A_i = \sum_i Y_i A_i, \quad i = 1, 2 \tag{4}$$

where A_i and Y_i are the cross-section and neutral axis of each layer, respectively. So, P is defined as

$$\begin{aligned} &P(t_1 n w_c + t_2 w_c) = \left(\frac{t_1}{2}\right)t_1 n w_c + \left(\frac{t_2}{2} + t_1\right)t_2 w_c \quad \Longrightarrow \\ &P = \frac{(\frac{t_1}{2})t_1 n + (\frac{t_2}{2} + t_1)t_2}{t_1 n + t_2}. \end{aligned} \tag{5}$$

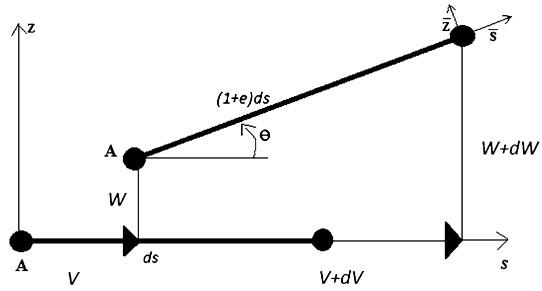

Fig. 3 A segment on the microbeam before and after deformation in fixed and local coordinate systems

And so

$$P = \frac{E_2 t_2 (t_1 + t_2)}{2(E_1 t_1 + E_2 t_2)}. \tag{6}$$

Because of the viscoelastic characteristics of the microbeam, a classical linear viscoelastic model, i.e., Kelvin–Voigt model is implemented:

$$\sigma_1 = E_1 \varepsilon_s + \hat{C} \dot{\varepsilon}_s \tag{7}$$

where σ_1 is the axial stress of the microbeam, ε_s is the strain, and $\hat{C}$ is the viscoelastic damping coefficient. Also, the stress–strain relationship for one directional piezoelectric material can be written as (Preumont 1997)

$$\sigma_2 = E_2 \varepsilon_s - E_2 d_{31} \frac{v_P}{t_2} \tag{8}$$

where σ_2 is the axial stress of the piezoelectric layer and d_{31} is the piezoelectric strain constant that usually is negative.

Based on the nonlinear Euler–Bernoulli beam theory, the strain of the microbeam can be written in the form of (Nayfeh and Pai 2004)

$$\varepsilon_s = e - kP \tag{9}$$

where e is the axial strain and k is the curvature bending of the microbeam in the sz plane. In order to facilitate the use of numerical or analytical methods, the Taylor series expansion is used (Nayfeh and Pai 2004):

$$\begin{aligned} e &= \sqrt{\left(1 + V'\right)^2 + W'^2} - 1 = V' + \frac{1}{2} W'^2 - \frac{1}{2} V' W'^2 + \cdots, \\ k &= \theta' = \left(W' - V'W' + V'^2 W' - \frac{1}{3} W'^3 \right)' \end{aligned} \tag{10}$$

in which V and W are the mid-plane displacement of the microbeam in the x and y direction, respectively (Fig. 3).

Also the total potential energy of the system may be obtained as

$$U = \int_0^v \int_0^\varepsilon \sigma_1 \, d\varepsilon \, dv_1 + \int_0^v \int_0^\varepsilon \sigma_2 \, d\varepsilon \, dv_2 \tag{11}$$

where v_1 and v_2 are the length of microbeam and piezoelectric layers, respectively. Expanding Eq. (11) reduces to

$$\begin{aligned} V &= (1 - H_{l_1}) \int_0^L \int_{-\frac{t_1}{2}}^{\frac{t_1}{2}} \int_0^{\varepsilon} \sigma_1 w_c \, d\varepsilon \, dz \, ds + (H_{l_1} - H_{l_2}) \int_0^L \int_{-\frac{t_1}{2}-P}^{\frac{t_1}{2}-P} \int_0^{\varepsilon} \sigma_1 w_c \, d\varepsilon \, dz \, ds \\ &\quad + (H_{l_1} - H_{l_2}) \int_0^L \int_{-\frac{t_1}{2}-P}^{\frac{t_1}{2}-P+t_2} \int_0^{\varepsilon} \sigma_2 w_c \, d\varepsilon \, dz \, ds + H_{l_2} \int_0^L \int_{-\frac{t_1}{2}}^{\frac{t_1}{2}} \int_0^{\varepsilon} \sigma_1 w_c \, d\varepsilon \, dz \, ds. \end{aligned} \tag{12}$$

Substituting Eqs. (7), (8) and (9) into Eq. (12) and considering Eq. (6), the potential energy of the system may be expressed as

$$\begin{aligned} V &= \frac{1}{2} \int_0^L B_1(s) e^2 \, ds - \int_0^L B_2(s) v_P e \, ds + \frac{1}{2} \int_0^L B_3(s) k^2 \, ds - \int_0^L B_4(s) v_P k \, ds \\ &\quad + \int_0^L B_5(s) e \dot{e} \, ds + \int_0^L B_6(s) k \dot{k} \, ds. \end{aligned} \tag{13}$$

Furthermore, the external force of the system which is due to the electrostatic actuation can be written as

$$F = \int_0^L Q w \, ds \tag{14}$$

where Q is the electrostatic force expressed as follows:

$$Q = -\frac{1}{2} \varepsilon_0 w_c \frac{(v_{\mathrm{dc}} + v_{\mathrm{ac}} \cos(\hat{\Omega} t))^2}{(h + W)^2} \tag{15}$$

where ε_0 is dielectric constant of the medium and h is the capacitor gap. Also, in this equation the fringing field effect of the electric field is neglected. According to Hamilton's principle, we have

$$\int_{t_1}^{t_2} (\delta K - \delta U + \delta F) = 0. \tag{16}$$

Substituting Eqs. (1), (13) and (15) into Eq. (16), the equations of motion, neglecting terms over the third order nonlinearities, are obtained as

$$\begin{aligned} & M(s) \ddot{V} - \big(B_1(s) V'\big)' - \big(B_5(s) \dot{V}'\big)' \\ &\quad = \left(B_1(s) \left[\frac{1}{2} W'^2 - V' W'^2\right]\right)' - \left(B_2(s) v_P \left[1 - \frac{1}{2} W'^2 + V' W'^2\right]\right)' \\ &\qquad + \big(W'\big(B_3(s)\big[W' - V'W'\big]'\big)' - 2V'W'\big(B_3(s) W''\big)'\big)' \\ &\qquad + \big(B_4'(s) v_P \big[W' + 2V'^2 W' - 2V'W' - W'^3 - V'^3 W'\big]\big)' \\ &\qquad + \big(B_5(s)\big[W'\dot{W}' - \dot{V}' W'^2 - V'W'\dot{W}'\big]\big)' + \big(W'\big(B_6(s)\big[\dot{W}' - \dot{V}'W' - \dot{V}'\dot{W}'\big]'\big)' \\ &\qquad - 2V'W'\big(B_6(s) \dot{W}''\big)'\big)' \end{aligned} \tag{17}$$

and

$$\begin{aligned}
&\big(B_3(s)W''\big)'' + M(s)\ddot{W} + \big(B_6(s)\dot{W}''\big)'' \\
&\quad = \left(B_1(s)\left[V'W' + \frac{1}{2}W'^3 - W'V'^2\right]\right)' \\
&\qquad + B_5(s)\big(W'^2\dot{W}' + \dot{V}'W' - \dot{V}'W'V'\big) + \Big(\big(B_3(s)\big(W'V'\big)'\big)'\big(1 - V'\big) \\
&\qquad + \big(W'^2 + V' - V'^2\big)\big(B_3(s)W''\big)' - \left(B_3(s)\left[V'^2W' - \frac{1}{3}W'^3\right]'\right)'\Big)' \\
&\qquad - \big(B_2(s)v_P\big(W' - W'V'\big)\big)' - \big(\big(B_4'(s)v_P\big(1 - V' - W'^2 - 3V'W'^2\big)\big)' \\
&\qquad + \big(B_6(s)\big[V'\dot{W} + \dot{V}'W'\big]'\big)'\big(1 - V'\big) + \big(B_3(s)\dot{W}''\big)'\big[V' - V'^2 + W'^2\big] \\
&\qquad - \big(B_3(s)\big[V'^2\dot{W}' + 2V'\dot{V}'W' - W'^2\dot{W}'\big]'\big)\big)' - \frac{1}{2}\varepsilon_0 w_c \frac{(v_{\mathrm{dc}} + v_{\mathrm{ac}}\cos(\hat{\Omega}t))^2}{(h+W)^2}
\end{aligned} \tag{18}$$

where

$$\begin{aligned}
&B_1(s) = (1 - H_{l_1})E_1A_1 + (H_{l_1} - H_{l_2})(E_1A_1 + E_2A_2) + H_{l_2}E_1A_1, \\
&B_2(s) = (H_{l_1} - H_{l_2})\frac{E_2A_2d_{31}}{t_2}, \\
&B_3(s) = (1 - H_{l_1})E_1I_1 + (H_{l_1} - H_{l_2})(E_1I_3 + E_2I_2) + H_{l_2}E_1I_1, \\
&B_4(s) = (H_{l_1} - H_{l_2})\frac{E_2A_3d_{31}}{t_2}, \\
&B_5(s) = (1 - H_{l_1})\bar{C}I_1 + (H_{l_1} - H_{l_2})\bar{C}I_3 + H_{l_2}E_1\bar{C}I_1, \\
&B_6(s) = \bar{C}A_1, \\
&A_1 = w_c t_1, \qquad A_2 = w_c t_2, \qquad A_3 = \frac{w_c}{2}\big(t_1t_2 + t_2^2 - 2t_2P\big), \\
&I_1 = \frac{w_c}{12}t_1^3, \qquad I_3 = \frac{w_c}{12}t_1^3 + t_1w_cP^2, \\
&I_2 = w_c\left(\left(\frac{1}{3}t_2^3\right) + \left(\frac{1}{2}t_1t_2^2\right) + \left(\frac{1}{4}t_2t_1^2\right) + t_2P^2 - \big(t_2^2 + t_1t_2\big)P\right).
\end{aligned} \tag{19}$$

For a slender beam, the longitudinal inertia in Eq. (17) may be negligible (Zamanian and Khadem 2008). Also based on the SI system of units, by considering the order of magnitude of the microbeam and piezoelectric thickness and the order of magnitude of the piezoelectric constant, according to Zamanian and Khadem (2008), $B_3(s)$ and $B_4(s)$ can be ignored when compared to $B_1(s)$ and $B_2(s)$. Also damping is negligible compared to stiffness in the longitudinal direction. To facilitate the extraction of the equation of motion, terms above the third order nonlinearities are ignored. By applying the above mentioned simplifications in

(17), one can obtain

$$\left(V'B_1(s)+\frac{1}{2}W'^2B_1(s)\right)'-B_3'(s)v_P=0. \tag{20}$$

Integrating Eq. (20) yields the following equation:

$$V'=-\frac{1}{2}W'^2+\frac{B_3(s)}{B_1(s)}v_P+\frac{B_c(t)}{B_1(s)}. \tag{21}$$

Equation (21) shows that the axial deformation is of the same order as of the quadratic transversal deformation, which means $O(V)=O(W^2)$.

Also $B_c(t)$ is the constant of integration that can be determined using the longitudinal boundary conditions:

$$v(0)=0, \qquad V(L)=\hat{f}. \tag{22}$$

So $B_c(t)$ becomes

$$B_c(t)=\frac{\hat{f}+\frac{1}{2}\int_0^L W'^2\,dx-\frac{E_2d_{31}A_2}{t_2(E_1A_1+E_2A_2)}v_P(l_2-l_1)}{\frac{l_1}{E_1A_1}+\frac{l_2-l_1}{E_1A_1+E_2A_2}+\frac{L-l_1}{E_1A_1}}. \tag{23}$$

Substituting V' from Eq. (21) into (18) by considering the mentioned simplifications, recalling that $O(V)=O(W^2)$, and keeping the terms up to cubic nonlinearities, the equation of transverse vibration of the microbeam is obtained as

$$\begin{aligned}
&\big(B_3(s)W''\big)''+\big(B_6(s)\dot{W}''\big)''+M(s)\ddot{W}\\
&\quad-B_5(s)\left(\frac{W'\int_0^L W'\dot{W}'ds}{B_1(s)(\frac{l_1}{E_1A_1}+\frac{l_2-l_1}{E_1A_1+E_2A_2}+\frac{L-l_1}{E_1A_1})}\right)\\
&\quad+\left(\frac{\hat{f}+\frac{1}{2}\int_0^L W'^2\,dx-\frac{E_2d_{31}A_2}{t_2(E_1A_1+E_2A_2)}v_P(l_2-l_1)}{\frac{l_1}{E_1A_1}+\frac{l_2-l_1}{E_1A_1+E_2A_2}+\frac{L-l_1}{E_1A_1}}W'\right)\\
&=\frac{1}{2}\varepsilon_0 w_c\frac{(v_{\mathrm{dc}}+v_{\mathrm{ac}}\cos(\hat{\Omega}t))^2}{(h+W)^2}.
\end{aligned} \tag{24}$$

It is easier to study and analyze the dimensionless form of this equation. So the nonlinear equation of motion can be rewritten in the dimensionless form as

$$\begin{aligned}
&\frac{\partial^2(H_{n1}(x)\frac{d^2w}{dx^2})}{\partial x^2}+M_n(x)\frac{d^2w}{dx^2}+C\frac{\partial^3}{\partial x^2\partial\tau}\left(H_{n2}(x)\frac{d^2w}{dx^2}\right)\\
&\quad-\big(\beta\Gamma(w_s,w_s)+\alpha-\gamma_{P1}v_P\big)\frac{d^2w}{dx^2}-2\beta C\Gamma\left(\frac{\partial w}{\partial\tau},w\right)\frac{\partial}{\partial x}\left(H_{n3}(x)\frac{\partial w}{\partial x}\right)\\
&=\frac{\eta(v_{\mathrm{dc}}+v_{\mathrm{ac}}\cos(\hat{\Omega}\tau))^2}{(1-w)^2}-\gamma_{P2}v_P\left(\frac{d^2H_{l_1/L}}{dx^2}-\frac{d^2H_{l_2/L}}{dx^2}\right),\\
&w|_{x=0}=0,\qquad \left.\frac{\partial w}{\partial x}\right|_{x=0}=0,\qquad w|_{x=1}=0,\qquad \left.\frac{\partial w}{\partial x}\right|_{x=1}=0.
\end{aligned} \tag{25}$$

Equation (25) is a dimensionless integral-partial-differential equation with linear and nonlinear terms. The dimensionless variables appearing in Eq. (25) are:

$$w=-\frac{W}{h}, \qquad x=\frac{s}{L}, \qquad \tau=\frac{t}{T}, \qquad T=\sqrt{\frac{\rho_1 t_1 w_c L^4}{E_1 I_1}}. \tag{26}$$

The parameters in the above equation are defined as follows:

$$\begin{aligned}
&\Gamma(a,b)=\int_0^L \frac{\partial a}{\partial x}\frac{\partial b}{\partial x}\,dx,\\
&M_n(x)=1+\frac{\rho_2 t_2}{\rho_1 t_1}(H_{l_1/L}-H_{l_2/L}),\\
&H_{n1}(x)=(1-H_{l_1/L})+\left(\frac{\bar{I}_1}{I_1}+\frac{E_2 I_2}{E_1 I_1}\right)(H_{l_1/L}-H_{l_2/L})+H_{l_2/L},\\
&H_{n2}(x)=(1-H_{l_1/L})+\frac{\bar{I}_1}{I_1}(H_{l_1/L}-H_{l_2/L})+H_{l_2/L},\\
&H_{n3}(x)=(1-H_{l_1/L})+\frac{E_1 A_1}{E_1 A_1+E_2 A_2}(H_{l_1/L}-H_{l_2/L})+H_{l_2/L},\\
&\alpha=\alpha_1\left(\frac{1+\frac{E_2 t_2}{E_1 t_1}}{(1+\frac{E_2 t_2}{E_1 t_1})(1-\frac{l_2-l_1}{L})+\frac{l_2-l_1}{L}}\right), \qquad \alpha_1=\frac{\hat{f} A_1 L}{I_1}, \qquad \Omega=\hat{\Omega}T,\\
&\beta=\beta_1\left(\frac{1+\frac{E_2 t_2}{E_1 t_1}}{(1+\frac{E_2 t_2}{E_1 t_1})(1-\frac{l_2-l_1}{L})+\frac{l_2-l_1}{L}}\right), \qquad \beta_1=6\left(\frac{h}{t_1}\right)^2,\\
&\eta=\frac{6\varepsilon_0 L^4}{E_1 t_1^3 h^3}, \qquad C=\frac{\hat{C}E_1}{T},\\
&\gamma_{P1}=\gamma_1\left(\frac{6(\frac{l_2-l_1}{L})\frac{E_2}{E_1}}{(1+\frac{E_2 t_2}{E_1 t_1})(1-\frac{l_2-l_1}{L})+\frac{l_2-l_1}{L}}\right), \qquad \gamma_1=\frac{2L^2 d_{31} v_P}{t_1^3},\\
&\gamma_{P2}=\gamma_2\left(\frac{E_2 t_2}{E_1 t_1}+\frac{E_2}{E_1}-\frac{(\frac{E_2}{E_1})^2\frac{t_2}{t_1}(1+\frac{t_2}{t_1})}{1+\frac{E_2 t_2}{E_1 t_1}}\right), \qquad \gamma_2=3\gamma_1\sqrt{\frac{6}{\alpha_1}};
\end{aligned} \tag{27}$$

α, β, η, C, γ_{P1}, and γ_{P2} are dimensionless parameters, which represent the axial load, mid-plane stretching, the electrostatic force, damping, piezoelectric axial force, and piezoelectric bending moment, respectively.

3 Governing equation of the static response

In order to extract the equation of the static response of the microbeam, terms with time derivatives, including inertia, damping, and variable forcing, have been assumed to be zero in Eq. (25). So, one obtains

$$\frac{\partial^2(H_{n1}(x)\frac{d^2w_s}{dx^2})}{\partial x^2} - \big(\beta\Gamma(w_s,w_s)+\alpha-\gamma_{P1}v_P\big)\frac{d^2w_s}{dx^2} = \frac{\eta v_{\mathrm{dc}}^2}{(1-w_s)^2} + \gamma_{P2}v_P\left(\frac{d^2H_{l_1/L}}{dx^2} - \frac{d^2H_{l_2/L}}{dx^2}\right), \tag{28}$$

$$w_s|_{x=0}=0, \qquad \left.\frac{\partial w_s}{\partial x}\right|_{x=0}=0, \qquad w_s|_{x=1}=0, \qquad \left.\frac{\partial w_s}{\partial x}\right|_{x=1}=0.$$

4 Governing equation of the dynamic response

For electrostatic actuation, first, the microbeam is deflected due to a DC voltage v_{dc} which is defined by $w_s(x)$ and then, the dynamic forced response of the system appears about this static equilibrium position which is defined by $u(x,t)$. So the total deflection of the microbeam consists of two parts as follows:

$$w(x,t) = w_s(x) + u(x,\tau). \tag{29}$$

Using Eq. (29) in Eq. (25), eliminating the static deflection terms represented by (28), and expanding the electrical term about the static position, the dynamic equation of motion of the microbeam is obtained:

$$\begin{aligned}&\frac{\partial^2(H_{n1}(x)\frac{\partial^2u}{\partial x^2})}{\partial x^2} + M_n(x)\frac{\partial^2u}{\partial\tau^2}\\ &\quad= \big(\beta\Gamma(w_s,w_s)+\alpha-\gamma_{P1}v_P\big)\frac{\partial^2u}{\partial x^2}\\ &\qquad+2\beta\Gamma(w_s,u)\frac{d^2w_s}{dx^2} + \beta\Gamma(u,u)\frac{d^2w_s}{dx^2} + 2\beta\Gamma(w_s,u)\frac{\partial^2u}{\partial x^2} + \beta\Gamma(u,u)\frac{\partial^2u}{\partial x^2}\\ &\qquad+\frac{2\eta v_{\mathrm{dc}}^2}{(1-w_s)^3}u + \frac{3\eta v_{\mathrm{dc}}^2}{(1-w_s)^4}u^2 + \frac{4\eta v_{\mathrm{dc}}^2}{(1-w_s)^5}u^3,\end{aligned} \tag{30}$$

$$u|_{x=0}=0, \qquad \left.\frac{\partial u}{\partial x}\right|_{x=0}=0, \qquad u|_{x=1}=0, \qquad \left.\frac{\partial u}{\partial x}\right|_{x=1}=0.$$

4.1 Linear eigenvalue problem

Eliminating nonlinear, damping and forcing terms from Eq. (30) and taking $u=\varphi(x)e^{i\omega\tau}$, the equation of the linear eigenvalue problem will be:

$$\begin{aligned}&\frac{d^2}{dx^2}\left(H_{1n}(x)\frac{d^2\varphi}{dx^2}\right) - \big(\beta\Gamma(w_s,w_s)+\alpha-\gamma_{P1}v_P\big)\frac{d^2\varphi}{dx^2} - 2\beta\Gamma(w_s,\varphi)\frac{d^2w_s}{dx^2}\\ &\quad-\left(\frac{2\eta v_{\mathrm{dc}}^2}{(1-w_s)^3}\right)\varphi = 0,\end{aligned} \tag{31}$$

$$\varphi|_{x=0}=0, \qquad \left.\frac{\partial\varphi}{\partial x}\right|_{x=0}=0, \qquad \varphi|_{x=1}=0, \qquad \left.\frac{\partial\varphi}{\partial x}\right|_{x=1}=0$$

where $\varphi(x)$ is the linear mode shape and ω is the natural frequency of the microbeam about its static deflection.

5 Static response of the system

In order to solve Eq. (28), the Galerkin method is implemented. So, w_s can be approximated as

$$w_s = \sum_{i=1}^{n} R_{s[i]}\varphi_{s[i]} \tag{32}$$

where $R_{s[i]}$ are unknown constants that would be obtained by applying the Galerkin method and $\varphi_{s[i]}$ is the ith undamped mode shape of a simple microbeam which is defined by:

$$\begin{aligned} &\frac{d^4\varphi_{s[i]}}{dx^4} - (\alpha - \gamma_{P1}v_P)\frac{d^2\varphi_{s[i]}}{dx^2} - (\Omega_{[i]})^2\varphi_{s[i]} = 0, \quad i = 1, 2, 3, \ldots, \\ &\left.\frac{d\varphi_{s[i]}}{dx}\right|_{x=0} = 0, \qquad \varphi_{s[i]}|_{x=0} = 0, \qquad \left.\frac{d\varphi_{s[i]}}{dx}\right|_{x=1} = 0, \qquad \varphi_{s[i]}|_{x=1} = 0. \end{aligned} \tag{33}$$

One can easily observe that Eq. (33) is the eigenvalue problem of a simple microbeam under axial loading $(\alpha - \gamma_{P1}v_P)$, $\varphi_{s[i]}$ is the ith mode shape, and $\Omega_{[i]}$ is the ith natural frequency of the system. This equation is a linear differential equation with constant coefficients. The characteristic equation for Eq. (33) can be obtained as

$$g^4 - (\alpha - \gamma_{P1}v_P)g^2 - (\Omega_{[i]})^2 = 0. \tag{34}$$

This equation has two complex conjugate roots:

$$\begin{aligned} g_1 &= \frac{1}{4}\sqrt{(\alpha - \gamma_{P1}v_P) + \sqrt{(\alpha - \gamma_{P1}v_P)^2 + 4(\Omega_{[i]})^2}}, \\ g_2 &= \frac{1}{4}\sqrt{-(\alpha - \gamma_{P1}v_P) + \sqrt{(\alpha - \gamma_{P1}v_P)^2 + 4(\Omega_{[i]})^2}}\, i \end{aligned} \tag{35}$$

where g_1, g_2 are the positive roots. The solution of Eq. (34) is expressed as:

$$\varphi_{s[i]} = C_1\cosh(g_1x) + C_2\sinh(g_1x) + C_3\sin(g_rx) + C_4\cos(g_rx) \tag{36}$$

where C_1, C_2, C_3 and C_4 are the coefficients that are obtained using boundary conditions. Also g_r is the real part of g_2.

Using Eq. (36) in (31), multiplying the resulting equation by $\varphi_{s[m]}$ and integrating the outcome from $x = 0$ to $x = 1$, a system of algebraic equations with variables $R_{s[i]}$ is obtained. Then, the coefficients $R_{s[i]}$ are calculated using numerical methods.

6 Natural frequencies of the system

In order to obtain the natural frequency of vibration for the deflected microbeam about its static position, the Galerkin method is used. So, it is assumed that

$$\varphi = \sum_{i=1}^{M} R_{d[i]}\varphi_{d[i]} \tag{37}$$

where $\varphi_{d[i]}$ is a comparison function that satisfies all boundary conditions. Considering some simplifications, the following equation with spring coefficient $2\eta v_{\mathrm{dc}}^2$ and axial load $(\beta\Gamma(w_s, w_s) + \alpha - \gamma_{P1} v_P)$ is used for obtaining comparison functions:

$$\begin{gathered} \frac{d^4\varphi_{d[i]}}{dx^4} - \big(\beta\Gamma(w_s, w_s) + \alpha - \gamma_{P1} v_P\big)\frac{d^2\varphi_{d[i]}}{dx^2} - \big(2\eta v_{\mathrm{dc}}^2 + \Omega_{1[i]}^2\big)\varphi_{d[i]} = 0, \\ \varphi_{d[i]}|_{x=0} = 0, \qquad \left.\frac{d\varphi_{d[i]}}{dx}\right|_{x=0} = 0, \qquad \varphi_{d[i]}|_{x=1} = 0, \qquad \left.\frac{d\varphi_{d[i]}}{dx}\right|_{x=1} = 0. \end{gathered} \tag{38}$$

The characteristic equation of Eq. (38) can be considered as

$$R^4 - \big(\beta\Gamma(w_s, w_s) + \alpha - \gamma_{P1} v_P\big)R^2 - \big(2\eta v_{\mathrm{dc}}^2 + \Omega_{1[i]}^2\big) = 0. \tag{39}$$

Equation (39) has four roots in which R_1 and R_2 are the positive roots:

$$\begin{aligned} R_1 &= \frac{1}{4}\sqrt{\big(\beta\Gamma(w_s, w_s) + \alpha - \gamma_{P1} v_P\big) + \sqrt{\begin{matrix}\big(\beta\Gamma(w_s, w_s) + \alpha - \gamma_{P1} v_P\big)^2 \\ + 4\big(\Omega_{1[i]}^2 + 2\eta v_{\mathrm{dc}}^2\big)\end{matrix}}}, \\ R_2 &= \frac{1}{4}\sqrt{-\big(\beta\Gamma(w_s, w_s) + \alpha - \gamma_{P1} v_P\big) + \sqrt{\begin{matrix}\big(\beta\Gamma(w_s, w_s) + \alpha - \gamma_{P1} v_P\big)^2 \\ + 4\big(\Omega_{1[i]}^2 + 2\eta v_{\mathrm{dc}}^2\big)\end{matrix}}}\, i. \end{aligned} \tag{40}$$

So, the solution of Eq. (38) is expressed as

$$\varphi_{d[i]} = X_1 \cosh(R_1 x) + X_2 \sinh(R_1 x) + X_3 \sin(R_r x) + X_4 \cos(R_r x) \tag{41}$$

where X_1, X_2, X_3 and X_4 are the coefficients that are obtained by applying the boundary conditions. Also R_r is the real part of R_2. Now, by using Eq. (41) in Eq. (37), multiplying the outcome by $\varphi_{d[m]}$ and integrating the result over the microbeam length from 0 to 1, $R_{d[i]}$ is obtained:

$$\begin{aligned} &\int_0^L \sum_{i=1}^M R_{d[i]}(1 - w_s)^3 \frac{d^2}{dx^2}\left(H_{n1}(x)\frac{d^2\varphi_{1[i]}}{dx^2}\right)\varphi_{d[m]}\,dx \\ &\quad - \int_0^L \sum_{i=1}^M R_{d[i]}(1 - w_s)^3\big(\beta\Gamma(w_s, w_s) + \alpha - \gamma_{P1} v_P\big)\frac{d^2\varphi_{1[i]}}{dx^2}\varphi_{d[m]}\,dx \\ &\quad - 2\beta\int_0^L \sum_{i=1}^M R_{d[i]}\Gamma(\varphi_{1[i]}, w_s)\varphi_{d[m]}\frac{d^2 w_s}{dx^2}(1 - w_s)^3\,dx \\ &\quad - \omega^2\int_0^L \sum_{i=1}^M R_{d[i]}M(x)(1 - w_s)^3\varphi_{1[i]}\varphi_{d[m]}\,dx - 2\eta v_{\mathrm{dc}}^2\int_0^L \sum_{i=1}^M R_{d[i]}\varphi_{1[i]}\varphi_{d[m]}\,dx = 0. \end{aligned} \tag{42}$$

By equating the determinant of the coefficients matrix to zero, the linear natural frequencies of the system can be obtained.

7 Primary resonance

In this section, the dynamic response of the system to the primary resonance excitation is investigated using the multiple scale method. First, a bookkeeping parameter ε is introduced to show the weakness of the nonlinear terms and fast and slow time scales $T_0 = \tau$, $T_1 = \varepsilon\tau$ and $T_2 = \varepsilon^2\tau$. Hence, the temporal operators can be expanded as:

$$\begin{aligned}
\frac{\partial}{\partial t} &= D_0 + \varepsilon D_1 + \varepsilon^2 D_2 + O(\varepsilon^3), \\
\frac{\partial^2}{\partial t^2} &= D_0^2 + 2\varepsilon D_0 D_1 + \varepsilon^2 D_1^2 + 2\varepsilon^2 D_0 D_2 + O(\varepsilon^3).
\end{aligned} \tag{43}$$

Also, $u(x, \tau)$ can be written as a third expansion in the form of

$$u(x, \tau) = \varepsilon u_1(x, T_0, T_1, T_2) + \varepsilon^2 u_2(x, T_0, T_1, T_2) + \varepsilon^3 u_3(x, T_0, T_1, T_2). \tag{44}$$

In order to balance the effect of nonlinearity, damping and forcing terms, C and v_{Ac} are replaced with $\varepsilon^2 C$ and $\varepsilon^3 v_{\mathrm{Ac}}$, respectively. Equating the coefficients of the same powers of ε leads to the following set of linear partial differential equations:

(Order ε^1)

$$\begin{aligned}
L(u_1) = {} & M_n(x)\frac{\partial^2 u_1}{\partial T_0^2} + \frac{\partial^2}{\partial x^2}\left(H_{n1}(x)\frac{\partial^2 u_1}{\partial x^2}\right) - \big(\beta\Gamma(w_s, w_s) + \alpha - \gamma_{P1} v_P\big)\frac{\partial^2 u_1}{\partial x^2} \\
& - 2\beta\Gamma(w_s, u_1)\frac{d^2 w_s}{dx^2} - \frac{2\eta v_{\mathrm{dc}}^2}{(1 - w_s)^3}u_1 = 0;
\end{aligned} \tag{45}$$

(Order ε^2)

$$L(u_2) = \beta\Gamma(u_1, u_1)\frac{d^2 w_s}{dx^2} + 2\beta\Gamma(w_s, u_1)\frac{d^2 u_1}{dx^2} + \frac{3\eta v_{\mathrm{dc}}^2}{(1 - w_s)^4}u_1^2 - 2M_n(x)\frac{\partial^2 u_1}{\partial T_0 \partial T_1}; \tag{46}$$

(Order ε^3)

$$\begin{aligned}
L(u_3) = {} & -2M_n(x)\frac{\partial^2 u_2}{\partial T_0 \partial T_1}\partial T - M_n(x)\left(\frac{\partial^2 u_1}{\partial T_1^2} + 2\frac{\partial^2 u_1}{\partial T_0 \partial T_2}\right) \\
& - C\frac{\partial^3}{\partial x^2 \partial T_0}\left(H_{n2}(x)\frac{\partial^2 u_1}{\partial x^2}\right) + 2\beta C\Gamma\left(\frac{\partial u_1}{\partial T_0}, w_s\right)\frac{\partial}{\partial x}\left(H_{n3}(x)\frac{dw_s}{dx}\right) \\
& + 2\beta\Gamma(u_1, u_2)\frac{d^2 w_s}{dx^2} + 2\beta\Gamma(w_s, u_2)\frac{\partial^2 u_1}{\partial x^2} + 2\beta\Gamma(w_s, u_1)\frac{\partial^2 u_2}{\partial x^2} \\
& + \beta\Gamma(u_1, u_1)\frac{\partial^2 u_1}{\partial x^2} + \frac{6\eta v_{\mathrm{dc}}^2}{(1 - w_s)^4}u_1 u_2 + \frac{4\eta v_{\mathrm{dc}}^2}{(1 - w_s)^5}u_1^3 \\
& + \frac{2\eta v_{\mathrm{dc}} v_{\mathrm{ac}} \cos(\Omega T_0)}{(1 - w_s)^4}.
\end{aligned} \tag{47}$$

The solution of Eq. (45) is

$$u_1(T_0, T_1, T_2) = A(T_1, T_2)e^{i\omega T_0}\phi(x) + \bar{A}(T_1, T_2)e^{-i\omega T_0}\phi(x) \tag{48}$$

where A and $\bar{A}$ are the complex amplitudes and their conjugates, respectively, that will be determined by applying the solvability condition at third order. The eigenfunction $\phi(x)$ describes normalized mode shapes so that $\int_0^1 \phi^2(x)\,dx = 1$.

By substituting Eq. (48) into Eq. (46),

$$\begin{aligned} L(u_2) = {} & \big(A^2 e^{2i\omega T_0} + 2A\bar{A} + \bar{A}^2 e^{-2i\omega T_0}\big)h(x) - 2M_n(x)\omega i\bigg(\frac{\partial A(T_1, T_2)}{\partial T_1}e^{i\omega T_0} \\ & - \frac{\partial \bar{A}(T_1, T_2)}{\partial T_1}e^{-i\omega T_0}\bigg) \end{aligned} \tag{49}$$

where

$$h(x) = \beta\Gamma(\phi, \phi)\frac{d^2 w_s}{dx^2} + 2\beta\Gamma(w_s, \phi)\frac{d^2\phi}{dx^2} + \frac{3\eta v_{\mathrm{dc}}^2}{(1 - w_s)^4}\phi^2. \tag{50}$$

The particular solution of Eq. (49) may be expressed as

$$u_2(T_0, T_2) = \psi_1(x)A^2 e^{2i\omega T_0} + 2\psi_2(x)A\bar{A} + \psi_1(x)\bar{A}^2 e^{-2i\omega T_0} \tag{51}$$

where $\psi_1(x)$ and $\psi_2(x)$ are the solutions of the boundary value problem,

$$\begin{aligned} & \frac{d^2}{dx^2}\bigg(H_{n1}(x)\frac{d^2\psi_i}{dx^2}\bigg) - 4\omega^2\delta_{1i}M_n(x)\psi_1 - \big(\beta\Gamma(w_s, w_s) + \alpha - \gamma_{P1}v_P\big)\frac{d^2\psi_i(x)}{dx^2} \\ & \quad - 2\beta\Gamma(w_s, \psi_i)\frac{d^2 w_s}{dx^2} - \frac{2\eta v_{\mathrm{dc}}^2}{(1 - w_s)^3}\psi_i = h(x), \\ & \psi_i|_{x=0} = 0, \qquad \frac{\partial\psi_i}{\partial x}\bigg|_{x=0} = 0, \qquad \psi_i|_{x=1} = 0, \qquad \frac{\partial\psi_i}{\partial x}\bigg|_{x=1} = 0. \end{aligned} \tag{52}$$

In Eq. (52), δ_{1i} is the Kronecker delta. Implementing Galerkin method and using the linear symmetric mode shapes of the deflected microbeam about its static position as comparison functions, the solution of Eq. (52) can be obtained.

Substituting Eqs. (48) and (51) into Eq. (47), replacing Ω by $\omega + \varepsilon^2\sigma$, where σ is a detuning parameter to express the nearness of the excitation frequency to the natural frequency, yields

$$\begin{aligned} L(u_3) = {} & \bigg[-2\omega i\frac{dA}{dT_2}M_n(x)\phi(x) - i\omega AC\chi^{\upsilon} + \chi(x)A^2\bar{A} + \bar{F}(x)e^{i\sigma T_2}\bigg]e^{i\omega T_0} + c.c. \\ & + N.S.T. \end{aligned} \tag{53}$$

where $c.c.$ indicates complex conjugate of the preceding terms and $N.S.T.$ means the other terms that do not produce secular terms. Also

$$\begin{aligned} \chi^{\upsilon} &= C\frac{d^2}{dx^2}\bigg(H_{n2}(x)\frac{d^2\phi}{dx^2}\bigg) - 2\beta C\Gamma(\phi, w_s)\frac{d}{dx}\bigg(H_{n3}(x)\frac{dw_s}{dx}\bigg), \\ \bar{F}(x) &= \frac{\eta v_{\mathrm{dc}} v_{\mathrm{ac}}}{(1 - w_s)^2}. \end{aligned} \tag{54}$$

The function $\chi(x)$ is defined as

$$\chi(x) = \chi_q^g + \chi_c^g + \chi_q^e + \chi_c^e \tag{55}$$

where χ_q^g and χ_c^g are the quadratic and cubic geometric nonlinear terms and χ_q^e and χ_c^e are the quadratic and cubic electric nonlinear terms, respectively, which are defined as:

$$\begin{aligned}
\chi_q^g &= \big(2\alpha_1 \Gamma(\psi_1, \phi) + 4\alpha_1 \Gamma(\psi_2, \phi)\big) \frac{d^2 w_s}{dx^2} + \left(2\alpha_1 \frac{d^2\psi_1}{dx^2} + 4\alpha_1 \frac{d^2\psi_2}{dx^2}\right) \Gamma(w_s, \phi) \\
&\quad + \big(2\alpha_1 \Gamma(\psi_1, w_s) + 4\alpha_1 \Gamma(\psi_2, w_s)\big) \frac{d^2\phi}{dx^2}, \\
\chi_q^e &= \frac{6\eta v_{\mathrm{dc}}^2}{(1-w_s)^4} (2\phi\psi_2 + \phi\psi_1), \\
\chi_c^g &= 3\beta \Gamma(\phi, \phi) \frac{d^2\phi}{dx^2}, \\
\chi_c^e &= \frac{12\eta v_{\mathrm{dc}}^2}{(1-w_s)^5} \phi^3.
\end{aligned} \tag{56}$$

The left-hand side of Eq. (53) is self-adjoint. So, the inhomogeneous equation (53) has a solution if the right-hand side of this equation is orthogonal to every solution of the corresponding homogeneous self-adjoint equation, that is, $\phi(x)e^{i\omega T_0}$. So, the solvability condition would be obtained by multiplying the right-hand side of inhomogenous equation (53) to $\phi(x)e^{i\omega T_0}$ and then, integrating the outcome from $x = 0$ to $x = 1$ as

$$2i\omega\left(\bar{M}\frac{dA}{dT_2} + \frac{\mu A}{2}\right) + 8SA^2\bar{A} - Fe^{i\sigma T_2} = 0 \tag{57}$$

where

$$\begin{aligned}
S &= S_q^g + S_c^g + S_q^e + S_c^e, \\
S_q^g &= -\frac{1}{8}\int_0^L \chi_q^g \phi\, dx, \\
S_c^g &= -\frac{1}{8}\int_0^L \chi_c^g \phi\, dx, \\
S_q^e &= -\frac{1}{8}\int_0^L \chi_q^e \phi\, dx, \\
S_c^e &= -\frac{1}{8}\int_0^L \chi_c^e \phi\, dx, \\
\mu &= C\int_0^L \chi^{v} \phi\, dx, \\
\bar{M} &= \int_0^L M_n(x)\phi^2\, dx, \\
F &= \int_0^L \bar{F}\phi\, dx = \int_0^L \frac{\eta v_{\mathrm{dc}} v_{\mathrm{ac}}}{(1-w_s)^2}\phi\, dx.
\end{aligned} \tag{58}$$

Expressing A in polar form gives

$$A = \frac{1}{2} a e^{i\vartheta} \tag{59}$$

where a and ϑ are amplitude and phase angle of the response, respectively. Considering $\vartheta = \sigma T_2 - \hat{\theta}$ and substituting Eq. (59) into (57), and splitting into real and imaginary parts, the following equations are obtained:

$$\begin{aligned} \bar{M} \frac{da}{dT_2} &= -\frac{\mu}{2} a + \frac{F}{\omega} \sin\hat{\theta}, \\ \bar{M} \frac{d\hat{\theta}}{dT_2} &= \sigma \bar{M} - \frac{S a^2}{\omega} + \frac{F}{a\omega} \cos\hat{\theta}. \end{aligned} \tag{60}$$

The point where $\frac{da}{dT_2} = 0$ and $\frac{d\hat{\theta}}{dT_2} = 0$ corresponds to a singular point of the system and shows its steady-state motion. So, in the steady-state condition this equilibrium criterion can be written as

$$a_0^2 \left(\left(\frac{\mu}{2} \right)^2 + \left(\sigma \bar{M} - \frac{S a_0^2}{\omega} \right)^2 \right) = \frac{F^2}{\omega^2}. \tag{61}$$

Equation (61) shows that the amplitude a_0 is maximum when term $(\sigma \bar{M} - \frac{S a_0^2}{\omega})^2$ is equal to zero, and so

$$\sigma = \frac{S a_0^2}{\omega \bar{M}}. \tag{62}$$

As a result, the maximum a_0 will be

$$a_0 = \frac{2F}{\omega \mu}. \tag{63}$$

Finally, the nonlinear resonance frequency is obtained as

$$\Omega = \omega + \frac{4 S F^2}{\bar{M} \omega^3 \mu^2}. \tag{64}$$

At last, solving Eq. (61) for σ yields

$$\sigma = \pm \frac{1}{a_0} \sqrt{\left(\frac{F^2}{\omega^2} - \mu^2 a_0^2 \right)} + \frac{S a_0^2}{\omega}. \tag{65}$$

8 Results and discussion

Numerical values which are used in the analysis are listed in Table 1. Also dimensionless values, in accordance to Table 1, are shown in Table 2. It is necessary to note that in this paper a (10, 10) SWNT was selected as a reinforcement and polymethyl methacrylate (PMMA) was used as a matrix material because of its good variable-climate-resisting property. The elastic modulus of CNT/PMMA nanocomposite was estimated by the Eshelby–Mori–Tanaka method (Chen and Cheng 1996).

Table 1 Geometrical and material properties of the microbeam and piezoelectric layer

	Microbeam	Piezoelectric layer
Length	200 μm	200 μm
Width	20 μm	20 μm
Thickness	1.5 μm	0.15 μm
Young's modulus	166 GPa	78.6 GPa
Mass density	$2331\ \mathrm{kg\,m^{-3}}$	$7500\ \mathrm{kg\,m^{-3}}$
Piezoelectric coefficient	–	$-9.29\ \mathrm{C\,m^{-2}}$
Initial gap	1.18 μm	–
Damping coefficient	$0.001\ \mathrm{Ns/m^2}$	–

Table 2 Values of parameters

β_1	γ_1	t_2	α_1	η	$l_2 - l_1$	v_{ac}
3.7	−2	$0.1t_1$	8.7	2.95	L	0.02

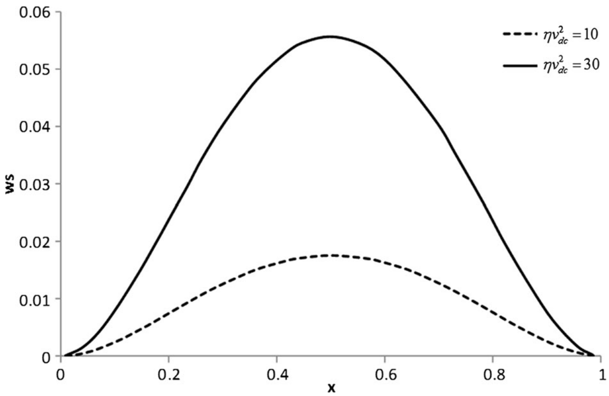

Fig. 4 Variations of static deflection with respect to x for $l_2 - l_1 = L$

For 28 % volume fraction of aligned (10, 10) SWNT fibers, and the aspect ratio of fibers greater than 1000, the elastic modulus of SWNT/PMMA nanocomposite is obtained as 166 GPa.

Neglecting the viscoelastic effects of the structure, the results of this work are compared with those of Zamanian and Khadem (2008, 2010) for the static deflection and frequency response, respectively, and good agreement between the results is obtained. They are shown in Figs. 5 and 16.

Figure 4 shows the variation of the static deflection of the microbeam with respect to polarization voltage. It is shown that, considering the boundary condition of the system, the maximum static response occurred in the center of the microbeam and it increased as v_{dc} increased.

Figure 5 shows the variation of the static deflection with electrostatic voltage, for this work and that of Zamanian and Khadem (2008), and represents a good agreement. In this comparison, it is considered that the piezoelectric layer covered 0.8 length of the microbeam and that the viscoelastic effect of the microbeam is eliminated.

Fig. 5 Comparison of the effect of ηv_{dc}^2 on the central static deflection for this work and that of Zamanian and Khadem (2008)

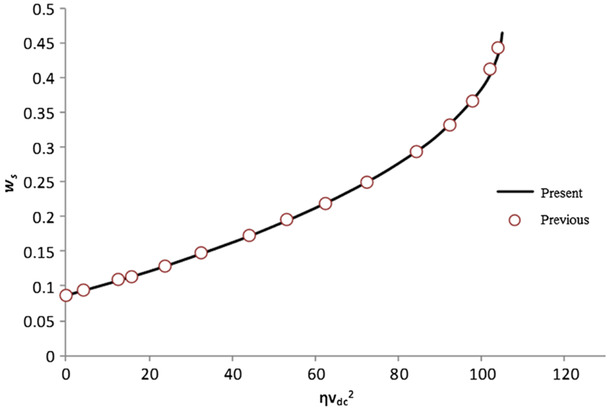

Fig. 6 Effect of ηv_{dc}^2 on the central static deflection microbeam for different piezoelectric layer length

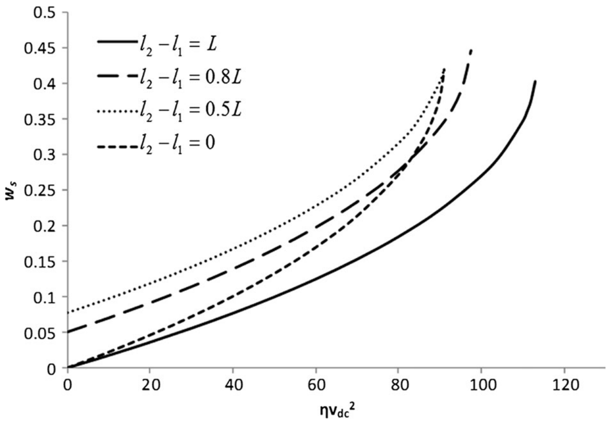

Figure 6 shows the variation of the static response with different lengths of the piezoelectric patch. It is necessary to note that in the corresponding equation, the effects of the nonlinear geometrical, electrostatic and piezoelectric terms have been considered. It is observed that for a constant piezoelectric length, the static deflection is increased as the electrostatic voltage is increased. By increasing the length of the piezoelectric layer from 0 to $0.5L$, for a constant value of ηv_{dc}^2, the static deflection is increased and, from $0.5L$ to L, it is decreased. Because of the piezoelectric layer effects in Eq. (28), static behavior of the microbeam changes for different length of the piezoelectric layer.

Considering Eq. (27), by increasing the length of the piezoelectric layer, $\gamma_{P1} v_P$ increases. Also Eq. (28) illustrates that the term $\gamma_{P2} v_P$ for $l_2 - l_1 = L$ and $l_2 - l_1 = 0$ goes to zero. So, decreasing the piezoelectric length causes the system stiffness to decrease and the microbeam deflection to increase. As a result, for the electrostatic voltage far from pull-in voltage, by decreasing the length of the piezoelectric layer from L to $0.5L$, the static deflection is increased. Also it is shown that the pull-in voltage for different length of the piezoelectric layer is varied, but, this phenomenon occurs for the deflection about $w_s \approx 0.4$. Also, it is shown that for the microbeam without a piezoelectric layer, due to lower stiffness of the system, the microbeam response became unstable for lower electrostatic voltage and so, pull-in occurred sooner.

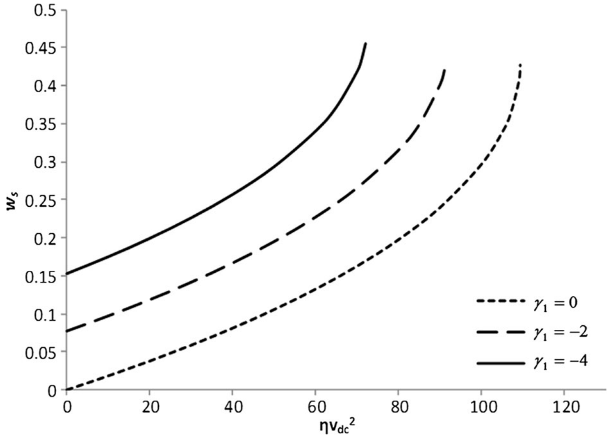

Fig. 7 Effect of ηv_{dc}^2 on the central static deflection microbeam for different γ_1

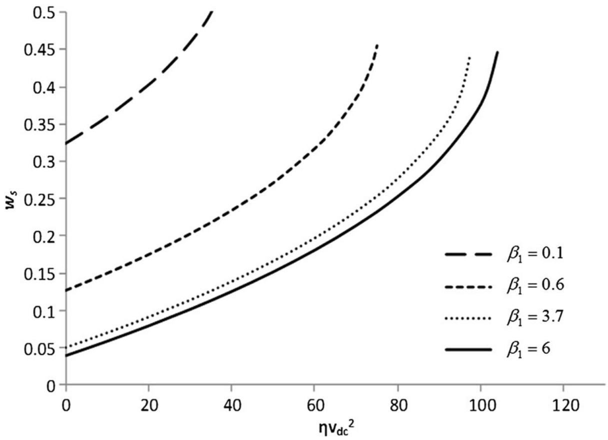

Fig. 8 Effect of ηv_{dc}^2 on the central static deflection microbeam for different β_1

Figure 7 shows the maximum static deflection of the microbeam for different values of γ_1. Increasing the piezoelectric voltage causes the static deflection to increase and the pull-in voltage to decrease. Also, it is shown that the static deflection has a nonzero value for $\eta v_{\mathrm{dc}}^2 = 0$, and is increased as the absolute value of γ_1 is increased.

In Fig. 8, the maximum static deflection of the microbeam for different values of β_1 is investigated. It is shown that by increasing β_1 the static deflection of the microbeam is decreased. As β_1 increased, the stiffness of the system also increased due to increasing the mid-plane stretching and so, the static deflection is decreased. Also it is observed that a lower β_1 leads to the sooner pull-in instability.

Figure 9 shows the effect of γ_1 on the static deflection of the microbeam for $l_2 - l_1 = 0.5L$. It is shown that by increasing the absolute value of γ_1, which means the increase of piezoelectric voltage for a microbeam with piezoelectric layer $l_2 - l_1 = 0.5L$, the static deflection is continuously increased. This happened due to terms with coefficients of $\gamma_{P1} v_P$ and $\gamma_{P2} v_P$ in the static equation (28).

Figure 10 shows the effect of β_1 on the static deflection of the microbeam for $l_2 - l_1 = 0.8L$. Considering Eq. (27), it is demonstrated that the maximum deflection occurs for the minimum stretching of the neutral axis. It is shown that by increasing β_1 the static deflection

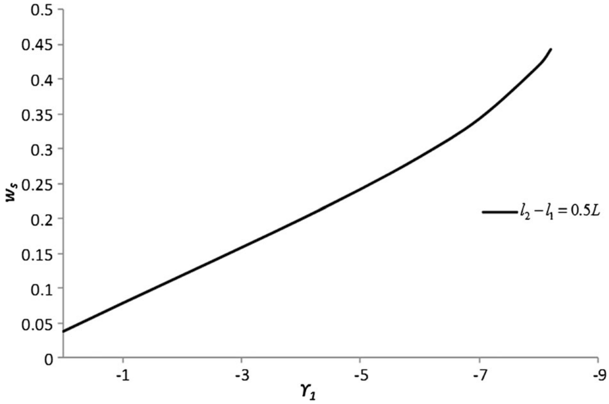

Fig. 9 Effect of γ_1 on the central static deflection microbeam with piezoelectric layer length equal to $l_2 - l_1 = 0.5L$

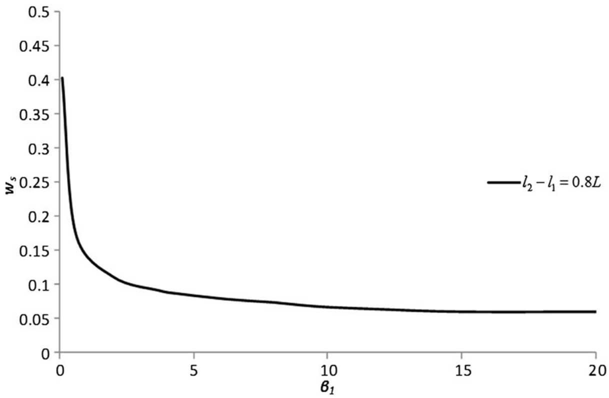

Fig. 10 Effect of β_1 on the central static deflection microbeam with piezoelectric layer length equal to $l_2 - l_1 = 0.8L$

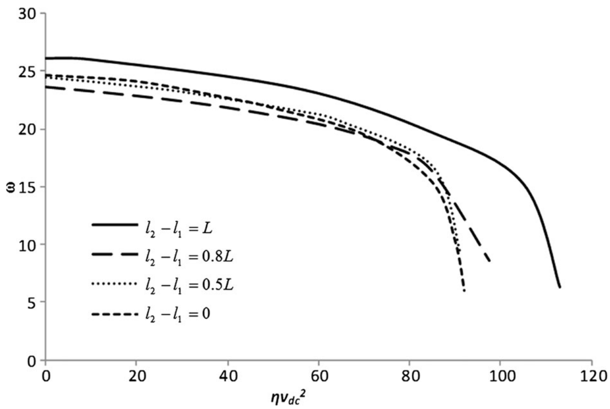

Fig. 11 Effect of ηv_{dc}^2 on the natural frequency of microbeam for different piezoelectric layer length

of the system is suddenly decreased and after that, increasing β_1 has only a small effect on the static deflection.

Figure 11 shows the variations of natural frequency of the system with respect to ηv_{dc}^2 for different lengths of the piezoelectric layer. It is shown that by increasing the length of

Fig. 12 Effect of ηv_{dc}^2 on the natural frequency of microbeam for different γ_1

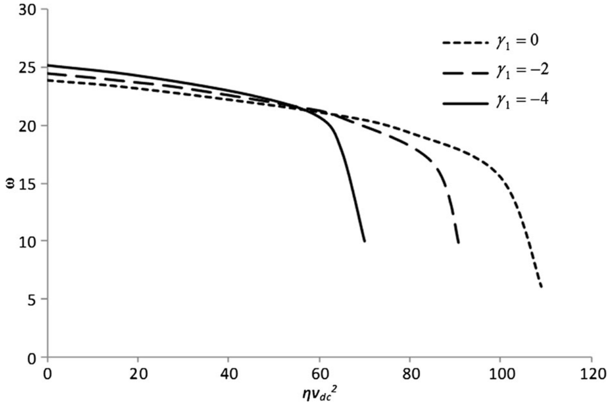

Fig. 13 Effect of ηv_{dc}^2 on the natural frequency of microbeam for different β_1

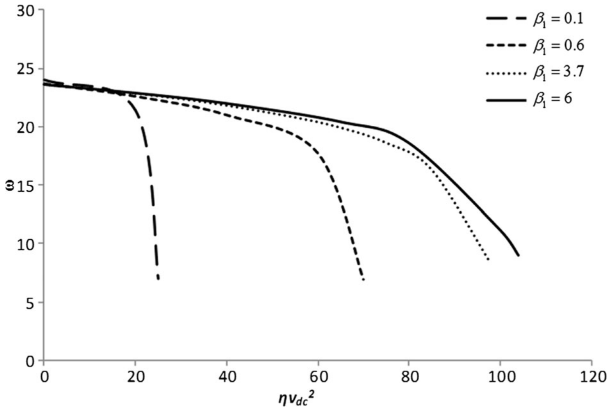

the piezoelectric layer from 0 to $0.8L$, the natural frequency is decreased, and for $0.8L$ to L is increased.

Figures 12 and 13 show the variations of the natural frequency of the system relative to ηv_{dc}^2. It is shown that, for a constant ηv_{dc}^2 far from the pull-in voltage, as the absolute value of γ_1 is increased, the natural frequency of the system is decreased, but, as the absolute value of β_1 is increased, the natural frequency of the system is increased.

The effects of γ_1 and β_1 on the natural frequency of the system are shown in Figs. 14 and 15, respectively. It is shown that by increasing γ_1 or β_1 the natural frequency of the system is increased.

Figure 16 shows the frequency response of the elastic system with a complete piezoelectric layer for $\eta v_{dc}^2 = 20$ which is compared to Zamanian and Khadem (2010), and a good and favorable agreement is obtained.

Figure 17 shows the variations of the vibration amplitude with respect to the detuning parameter σ. According to Eq. (61), the frequency response of the system depends on the various system parameters. All these parameters are positive except for S which can be positive or negative. S contains the nonlinear stiffness terms that include geometry, piezoelectric and electrostatic nonlinearities. For $S > 0$, according to Eq. (64), the nonlinear resonance frequency becomes greater than the linear one, i.e., $\frac{\Omega}{\omega} > 1$. This causes the hardening behavior of the system. In the same manner, for $S < 0$ the nonlinear resonance frequency is lower than the linear one and the softening behavior appears. As shown in Fig. 17, by increas-

Fig. 14 Effect of γ_1 on the natural frequency of microbeam with piezoelectric layer length equal to $l_2 - l_1 = 0.5L$

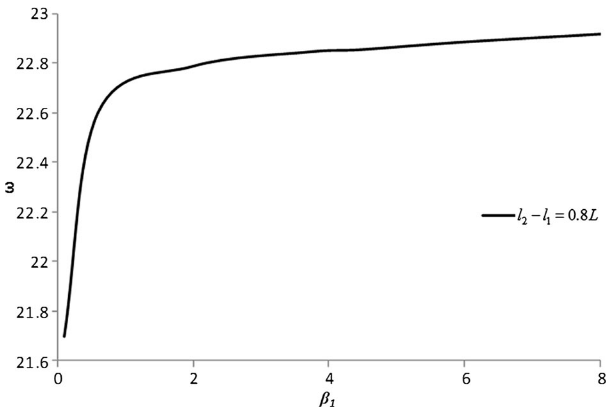

Fig. 15 Effect of β_1 on the natural frequency of microbeam with piezoelectric layer length equal to $l_2 - l_1 = 0.8L$

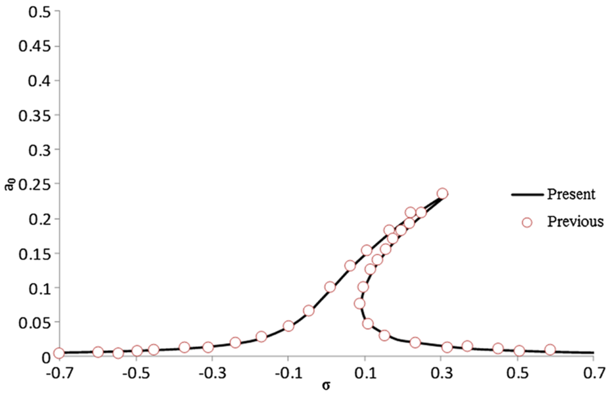

Fig. 16 Comparison between frequency response of this work with Zamanian and Khadem (2010) in $\eta v_{dc}^2 = 20$ with piezoelectric layer L

ing the electrostatic voltage, the system represents a more softening behavior. For constant piezoelectric parameters, increasing the electrostatic voltage reduces to decreasing S to negative values, and so, the softening behavior appears. Also, as ηv_{dc}^2 is increased, the vibration amplitude is increased, which is due to the increasing value of F in Eq. (58).

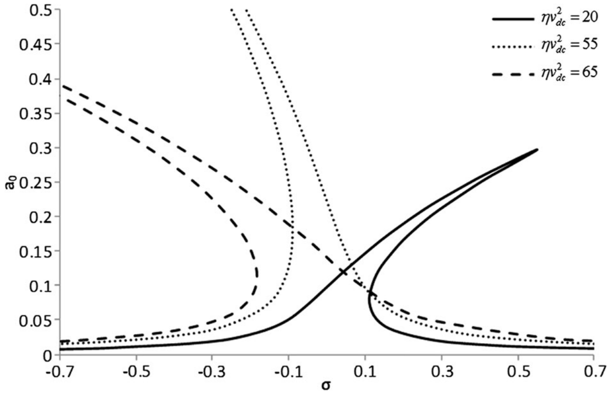

Fig. 17 Frequency response of microbeam for different actuation electrostatic voltage

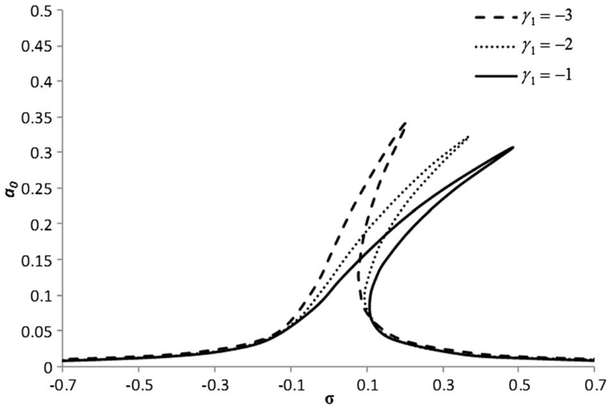

Fig. 18 Frequency response of microbeam for different γ_1

Figure 18 depicts the variation of the vibration amplitude relative to the detuning parameter σ. It is shown that increasing the absolute value γ_1 makes the system softer and, by tuning the value of γ_1, one can expect a linear response from a nonlinear system. Also, as shown in this figure, the amplitude of a nonlinear vibration is increased as the absolute value of γ_1 is increased. By increasing γ_1, the static deflection of the microbeam is increased and, according to Eqs. (28), (58) and (63), w_s, F and also a_0 are subsequently increased.

Figure 19 shows the effect of β_1 on the dynamic response of the microbeam. It is shown that increasing the value of β_1 leads to increasing the hardening behavior of the system. Increasing the value of β_1 causes the static deflection to decrease and the natural frequency of the system to increase, and so, according to Eq. (63), leads to a decreasing amplitude of the vibration.

Figure 20 shows the frequency response of the microbeam for different AC voltages. As shown in this figure, by increasing the AC voltage, according to Eqs. (58) and (63), the nonlinear vibration amplitude is increased, and the nonlinear resonance occurs at a higher excitation frequency. Also one can observe that the hardening state of the system remains unchanged due to the variation of v_{ac}.

The effect of the electrostatic voltage on the damping of the system is shown in Fig. 21. As shown in this figure, the damping characteristic of the system is increased as the electrostatic voltage is increased, especially near the pull-in voltage. So, one can say that for a viscoelastic microbeam, the damping of the system not only depends on the viscoelastic

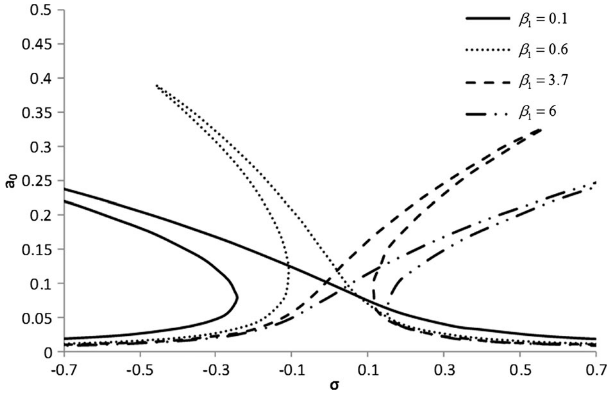

Fig. 19 Frequency response of microbeam for different β_1

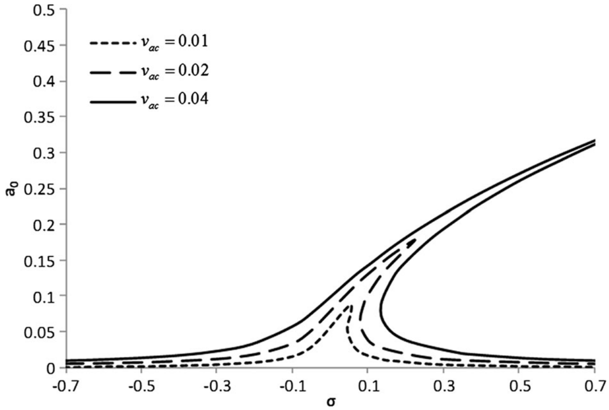

Fig. 20 Frequency response of microbeam for different AC voltage

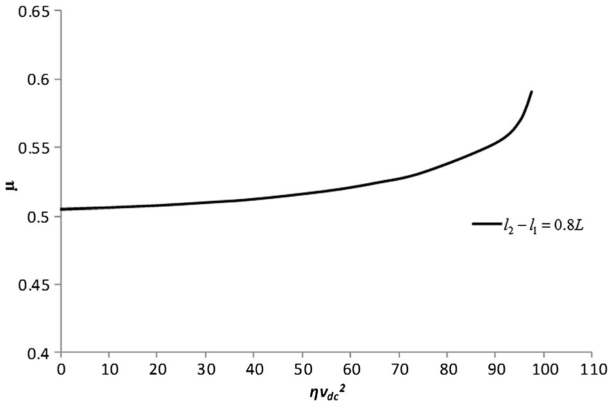

Fig. 21 Effect of ηv_{dc}^2 on the damping of system for $C = 0.001$

damping coefficient C, but also on other parameters of the system, for example, electrostatic voltage.

Figures 22 and 23 show the variation of the damping characteristics of the system to β_1 and γ_1, and one can easily observe that β_1 has no evident effect on the damping of the system. But, the damping characteristic is increased as γ_1 is increased.

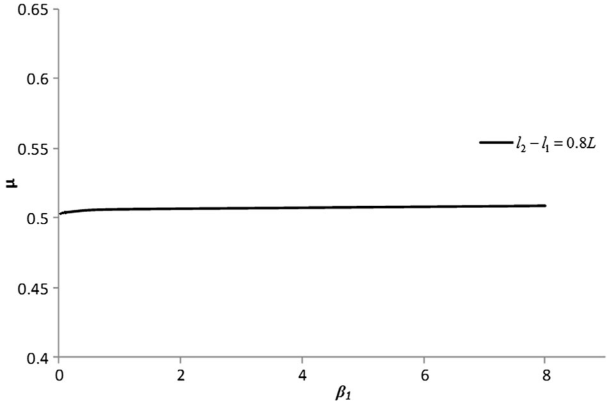

Fig. 22 Effect of β_1 on the damping of system for $C = 0.001$

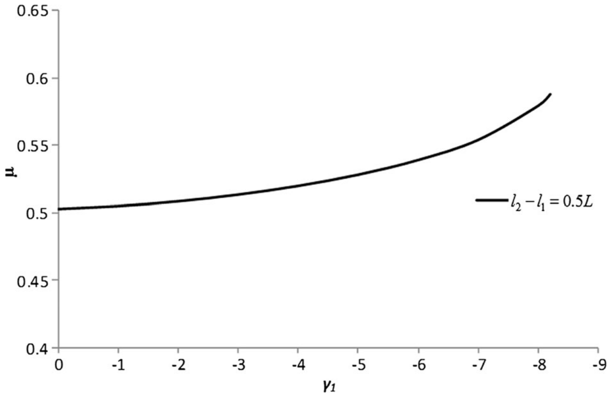

Fig. 23 Effect of γ_1 on the damping for $C = 0.001$

9 Conclusion

In this paper, the nonlinear dynamic response of a nanocomposite microbeam is studied under electric and piezoelectric actuations. The microbeam has been assumed as a clamped–clamped Euler–Bernoulli microbeam and having a symmetric piezoelectric patch deposited on it. The Galerkin method and a perturbation method are applied to solve the nonlinear equation of motion.

According to the obtained result, for a specific length of the piezoelectric, the hardening behavior occurs for lower values of the DC voltage in electrostatic actuation and, by increasing the value of this DC voltage, a softening behavior is detected. Also, for a piezoelectric actuation by increasing piezoelectric voltage values, a softening behavior is observed. At the same time, an increase of the mid-plane stretching causes a hardening of the system. Also it is shown that damping characteristics of the system depends on both damping coefficient C and on other parameters of the system.

References

Ashrafi, B., Hubert, P., Vengallatore, S.: Carbon nanotube-reinforced composites as structural materials for microactuators in microelectromechanical systems. Nanotechnology **17**, 4895–4903 (2006)

Chen, C.H., Cheng, C.H.: Effective elastic moduli of misoriented short-fiber composites. Int. J. Solids Struct. **33**, 2519–2539 (1996)

Chen, C., Hu, H., Dai, L.: Nonlinear behavior and characterization of a piezoelectric laminated microbeam system. Commun. Nonlinear Sci. Numer. Simul. **18**, 1304–1315 (2013)

Fu, Y.M., Zhang, J.: Active control of the nonlinear static and dynamic responses for piezoelectric viscoelastic microplates. Smart Mater. Struct. (2009). doi:10.1088/0964-1726/18/9/095037

Fu, Y.M., Zhang, J., Bi, R.G.: Analysis of the nonlinear dynamic stability for an electrically actuated viscoelastic microbeam. Microsyst. Technol. **15**, 763–769 (2009)

Ghayesh, M.H., Amabili, M., Farokhi, H.: Nonlinear forced vibrations of a microbeam based on the strain gradient elasticity theory. Int. J. Eng. Sci. **63**, 52–60 (2013a)

Ghayesh, M.H., Farokhi, H., Amabili, M.: Nonlinear behaviour of electrically actuated MEMS resonators. Int. J. Eng. Sci. **71**, 137–155 (2013b)

Ghazavi, M.R., Rezazadeh, G., Azizi, S.: Pure parametric excitation of a micro cantilever beam actuated by piezoelectric layers. Appl. Math. Model. **34**, 4196–4207 (2010)

Hosseinzadeh, A., Ahamadian, M.T.: Application of piezoelectric and functionally graded materials in designing electrostatically actuated micro switches. J. Solid Mech. **2**, 179–189 (2010)

Jalali, A., Khadem, S.E.: Pull-in analysis of a nonlinear viscoelastic nanocomposite microplate under an electrostatic actuation. J. Mech. **28**, 179–189 (2010)

Kacem, N., Baguet, S., Hentz, S., Dufour, R.: Computational and quasi-analytical models for non-linear vibrations of resonant MEMS and NEMS sensors. Int. J. Non-Linear Mech. **46**, 532–542 (2011)

Kim, P., Bae, S., Seok, J.: Resonant behaviors of a nonlinear cantilever beam with tip mass subject to an axial force and electrostatic excitation. Int. J. Mech. Sci. **64**, 232–257 (2012)

Mahmoodi, S.N., Jalili, N.: Non-linear vibrations and frequency response analysis of piezoelectrically driven microcantilevers. Int. J. Non-Linear Mech. **42**, 577–587 (2007)

Mojahedi, M., Moghimi Zand, M., Ahmadian, M.T.: Static pull-in analysis of electrostatically actuated microbeams using homotopy perturbation method. Appl. Math. Model. **34**, 1032–1041 (2010)

Nayfeh, A.H., Pai, P.F.: Linear and Nonlinear Structural Mechanics. Wiley, New York (2004)

Preumont, A.: Vibration Control of Active Structure: An Introduction. Kluwer Academic/Springer, Dordrecht (1997)

Qian, D., Wagner, G.J., Liu, W.K., Yu, F., Ruoff, R.S.: Mechanics of carbon nanotubes. Appl. Mech. Rev. **55**, 495–533 (2002)

Rezazadeh, G., Tahmasebi, A., Zubstov, M.: Application of piezoelectric layers in electrostatic MEM actuators: controlling of pull-in voltage. Microsyst. Technol. **12**, 1163–1170 (2006)

Rezazadeh, G., Fathalilou, M., Shabani, R.: Static and dynamic stabilities of a microbeam actuated by a piezoelectric voltage. Microsyst. Technol. **15**, 1785–1791 (2009)

Raeisifard, H., Bahrami, M.N., Yousefi, A., Raeisifard, H.: Static characterization and pull-in voltage of a micro-switch under both electrostatic and piezoelectric excitations. Eur. J. Mech. A, Solids **44**, 116–124 (2014)

Senturia, S.D.: Microsystem Design. Kluwer Academic, Norwell (2001)

Shooshtari, A., Hoseini, S.M., Mahmoodi, S.N., Kalhori, H.: Analytical solution for nonlinear free vibrations of viscoelastic microcantilevers covered with a piezoelectric layer. Smart Mater. Struct. **21** (2012). doi:10.1088/0964-1726/21/7/075015

Timoshenko, S.P.: Strength of Materials/Part 1, Elementary Theory and Problems, 2nd edn. Van Nostrand, Princeton (1940)

Younis, M.I.: MEMS Linear and Nonlinear Statics and Dynamics p. 276. Springer, New York (2011)

Zamanian, M., Khadem, S.E.: The effect of a piezoelectric layer on the mechanical behavior of an electrostatic actuated microbeam. Smart Mater. Struct. **17** (2008). doi:10.1088/0964-1726/17/6/065024

Zamanian, M., Khadem, S.E.: Nonlinear vibration of an electrically actuated microresonator tuned by combined DC piezoelectric and electric actuations. Smart Mater. Struct. **19** (12 pp.) (2010)

Zamanian, M., Mahmoodi, S.N., Khadem, S.E.: Nonlinear response of a resonant viscoelastic microbeam under an electrical actuation. Struct. Eng. Mech. **35**, 487–493 (2010)